

Reconstructing the Primordial Spectrum from WMAP Data by the Cosmic Inversion Method

Noriyuki Kogo¹, Makoto Matsumiya², Misao Sasaki³, and Jun'ichi Yokoyama⁴

^{1,2,4}*Department of Earth and Space Science, Graduate School of Science, Osaka University,
Toyonaka 560-0043, Japan*

³*Yukawa Institute for Theoretical Physics, Kyoto University, Kyoto 606-8502, Japan*

¹kogo@vega.ess.sci.osaka-u.ac.jp, ²matsumiya@vega.ess.sci.osaka-u.ac.jp,
³misao@yukawa.kyoto-u.ac.jp, ⁴yokoyama@vega.ess.sci.osaka-u.ac.jp

ABSTRACT

We reconstruct the primordial spectrum of the curvature perturbation, $P(k)$, from the observational data of the Wilkinson Microwave Anisotropy Probe (WMAP) by the cosmic inversion method developed recently. In contrast to conventional parameter-fitting methods, our method can potentially reproduce small features in $P(k)$ with good accuracy. As a result, we obtain a complicated oscillatory $P(k)$. We confirm that this reconstructed $P(k)$ recovers the WMAP angular power spectrum with resolution up to $\Delta\ell \simeq 5$. Similar oscillatory features are found, however, in simulations using artificial cosmic microwave background data generated from a scale-invariant $P(k)$ with random errors that mimic observation. In order to examine the statistical significance of the nontrivial features, including the oscillatory behaviors, therefore, we consider a method to quantify the deviation from scale-invariance and apply it to the $P(k)$ reconstructed from the WMAP data. We find that there are possible deviations from scale-invariance around $k \simeq 1.5 \times 10^{-2}$ and $2.6 \times 10^{-2} \text{Mpc}^{-1}$.

Subject headings: cosmic microwave background—cosmology: theory

1. Introduction

The Wilkinson Microwave Anisotropy Probe (WMAP) satellite has brought us interesting information about our universe (Bennett et al. 2003). From the remarkably precise observation of the temperature fluctuations and the polarization of the cosmic microwave

background (CMB), one can obtain not only accurate values of the global cosmological parameters, but also invaluable information of the properties on the primordial fluctuations (Bennett et al. 2003; Spergel et al. 2003; Peiris et al. 2003; Komatsu et al. 2003). Although their results as a whole support the standard Λ CDM (cold dark matter) model with Gaussian, adiabatic, and scale-invariant primordial fluctuations, some features that cannot be explained by the standard model have also been pointed out, such as (1) lack of power on large scales, (2) running of the spectral index n_s from $n_s > 1$ on larger scales to $n_s < 1$ on smaller scales, and (3) oscillatory behaviors of the power spectrum on intermediate scales.

In fact, feature 1 was known already with COBE data (Bennett et al. 1996), and a possible explanation was proposed (Yokoyama 1999). There have been many new proposals (Bi et al. 2003; de Deo et al. 2003; Efstathiou 2003a; Uzan et al. 2004; Contaldi et al. 2003; Cline et al. 2003; Feng and Zhang 2003; Kawasaki and Takahashi 2003; Dvali and Kachru 2003; Piao et al. 2003), as well as many arguments about its statistical significance (Spergel et al. 2003; Tegmark et al. 2003; de Oliveira-Costa et al. 2003; Gaztañaga et al. 2003; Niarchou et al. 2004; Efstathiou 2003b, 2004). A number of inflation models that can account for feature 2 have also been proposed recently (Feng et al. 2003; Kyae and Shafi 2003; Kawasaki et al. 2003; Huang and Li 2003; Chung et al. 2003; Yamaguchi and Yokoyama 2003; Dvali and Kachru 2003).

On the other hand, feature 3, namely, possible oscillatory behaviors around a simple power-law spectrum, is more difficult to quantify (Peiris et al. 2003). Although several attempts to reconstruct the primordial spectrum were made by combining WMAP data with other independent observational data, such as the Two-Degree Field Galaxy Redshift Survey (2dFGRS) and $\text{Ly}\alpha$ forest data (Wang et al. 1999a,b; Hannestad 2001, 2003; Tegmark and Zaldarriaga 2002; Wang and Mathews 2002; Bridle et al. 2003; Mukherjee and Wang 2003a,b,c), they all employed the binning, wavelet band powers, or direct wavelet expansion method to the data. These methods cannot detect possible oscillatory behaviors if their scale is smaller than the binning scale. It is preferable to use a method that can restore the primordial spectrum as a continuous function without any ad hoc filtering scale to investigate detailed features such as 3. Fortunately, such a new method has been proposed in Matsumiya et al. (2002) and Matsumiya et al. (2003), with the name cosmic inversion method, and their test calculations using mock data without observational errors have shown that this method can reproduce possible small dips and peaks off a scale-invariant spectrum quite well, in the spatially flat universe with the adiabatic initial condition. In this paper, we attempt to reconstruct $P(k)$ from the WMAP data using this method. To apply it to the actual data, we consider the observational errors by Monte Carlo simulations and use a modified

CMBFAST¹ code that adopts much finer resolution than the original one in both k and ℓ , so that we can compute the fine structure of angular power spectra accurately. We mention that recently another new method for the reconstruction of $P(k)$ has been proposed by Shafieloo and Souradeep (2003).

This paper is organized as follows. In Sec. 2, we review the cosmic inversion method and describe our analysis method using the WMAP data. In Sec. 3, we apply our method to the WMAP data and discuss the results. In particular, we investigate statistical significance of deviations from scale-invariance. Finally, we present our conclusion in Sec. 4.

2. Inversion Method

First, we briefly review the cosmic inversion method proposed by Matsumiya et al. (2002, 2003). We assume a spatially flat universe with an adiabatic initial condition, both of which are generic predictions of standard inflation and have been supported by the WMAP data. In the end, we obtain a first-order differential equation for the primordial spectrum $P(k)$.

The CMB anisotropy is quantified by the angular correlation function defined as

$$C(\theta) \equiv \langle \Theta(\hat{\mathbf{n}}_1) \Theta(\hat{\mathbf{n}}_2) \rangle = \sum_{\ell=0}^{\infty} \frac{2\ell+1}{4\pi} C_{\ell} P_{\ell}(\cos \theta), \quad \cos \theta = \hat{\mathbf{n}}_1 \cdot \hat{\mathbf{n}}_2, \quad (1)$$

where $\Theta(\hat{\mathbf{n}})$ is the temperature fluctuation in the direction $\hat{\mathbf{n}}$. We decompose the Fourier components of the temperature fluctuations $\Theta(\eta, k)$ into multipole moments,

$$\Theta(\eta, k, \mu) = \sum_{\ell=0}^{\infty} (-i)^{\ell} \Theta_{\ell}(\eta, k) P_{\ell}(\mu), \quad (2)$$

where $\mu \equiv \hat{\mathbf{k}} \cdot \hat{\mathbf{n}}$, k is the comoving wavenumber, and η is the conformal time, with its present value being η_0 . Using $\Theta_{\ell}(\eta, k)$, the angular power spectrum is expressed as

$$\frac{2\ell+1}{4\pi} C_{\ell} = \frac{1}{2\pi^2} \int_0^{\infty} \frac{dk}{k} \frac{k^3 \langle |\Theta_{\ell}(\eta_0, k)|^2 \rangle}{2\ell+1}. \quad (3)$$

The Boltzmann equation for $\Theta(\eta, k)$ can be transformed into the following integral form (Hu and Sugiyama 1995):

$$(\Theta + \Psi)(\eta_0, k, \mu) = \int_0^{\eta_0} d\eta \left\{ [\Theta_0 + \Psi - i\mu V_b] \mathcal{V}(\eta) + (\dot{\Psi} - \dot{\Phi}) e^{-\tau(\eta)} \right\} e^{ik\mu(\eta-\eta_0)}, \quad (4)$$

¹See <http://www.cmbfast.org/>

where the overdot denotes the derivative with respect to the conformal time. Here, Ψ and Φ are the Newton potential and the spatial curvature perturbation in the Newton gauge, respectively (Kodama and Sasaki 1984), and

$$\mathcal{V}(\eta) \equiv \dot{\tau} e^{-\tau(\eta)}, \quad \tau(\eta) \equiv \int_{\eta}^{\eta_0} \dot{\tau} d\eta, \quad (5)$$

are the visibility function and the optical depth for Thomson scattering, respectively. In the limit that the thickness of the last scattering surface (LSS) is negligible, we have $\mathcal{V}(\eta) \approx \delta(\eta - \eta_*)$, $e^{-\tau(\eta)} \approx \theta(\eta - \eta_*)$, where η_* is the recombination time when the visibility function is maximum (Hu and Sugiyama 1995). Taking the thickness of the LSS into account, we have a better approximation for Eq. (4) as

$$(\Theta + \Psi)(\eta_0, k, \mu) \approx \int_{\eta_{*start}}^{\eta_{*end}} d\eta \left\{ [\Theta_0 + \Psi - i\mu\Theta_1] \mathcal{V}(\eta) + (\dot{\Psi} - \dot{\Phi}) e^{-\tau(\eta)} \right\} e^{-ik\mu d} \equiv \Theta^{app} + \Psi, \quad (6)$$

where $d \equiv \eta_0 - \eta_*$ is the conformal distance from the present to the LSS and η_{*start} and η_{*end} are the times when the recombination starts and ends, respectively. Here we introduce the transfer functions, $f(k)$ and $g(k)$, defined by

$$\int_{\eta_{*start}}^{\eta_{*end}} d\eta \left[(\Theta_0 + \Psi)(\eta, k) \mathcal{V}(\eta) + (\dot{\Psi} - \dot{\Phi})(\eta, k) e^{-\tau(\eta)} \right] \equiv f(k) \Phi(0, \mathbf{k}), \quad (7)$$

$$\int_{\eta_{*start}}^{\eta_{*end}} d\eta \Theta_1(\eta, k) \mathcal{V}(\eta) \equiv g(k) \Phi(0, \mathbf{k}). \quad (8)$$

We can calculate $f(k)$ and $g(k)$ numerically; they depend only on the cosmological parameters, for we are assuming that only adiabatic fluctuations are present. Then, we find the approximated multipole moments as

$$\Theta_\ell^{app}(\eta_0, k) = (2\ell + 1) [f(k) j_\ell(kd) + g(k) j'_\ell(kd)] \Phi(0, \mathbf{k}), \quad (9)$$

and the approximated angular correlation function as

$$C^{app}(r) = \sum_{\ell=\ell_{min}}^{\ell_{max}} \frac{2\ell + 1}{4\pi} C_\ell^{app} P_\ell \left(1 - \frac{r^2}{2d^2} \right), \quad (10)$$

where C_ℓ^{app} is obtained by putting Eq. (9) into Eq. (3), r is defined as $r = 2d \sin(\theta/2)$ on the LSS, and ℓ_{min} and ℓ_{max} are lower and upper bounds on ℓ due to the limitation of the observation. In the small-scale limit $r \ll d$, using the Fourier sine formula, we obtain a first-order differential equation for the primordial power spectrum of the curvature perturbation, $P(k) \equiv \langle |\Phi(0, \mathbf{k})|^2 \rangle$,

$$\begin{aligned} & -k^2 f^2(k) P'(k) + [-2k^2 f(k) f'(k) + k g^2(k)] P(k) \\ & = 4\pi \int_0^\infty dr \frac{1}{r} \frac{\partial}{\partial r} \{ r^3 C^{app}(r) \} \sin kr \equiv S(k). \end{aligned} \quad (11)$$

Since $f(k)$ and $g(k)$ are oscillatory functions around zero, we can find values of $P(k)$ at the zero points of $f(k)$ as

$$P(k_s) = \frac{S(k_s)}{k_s g^2(k_s)} \quad \text{for } f(k_s) = 0, \quad (12)$$

assuming that $P'(k)$ is finite at the singularities, $k = k_s$. If the cosmological parameters and the angular power spectrum are given, we can solve Eq. (11) as a boundary value problem between the singularities.

However, because Eq. (11) is derived by adopting the approximation in Eq. (6), C_ℓ^{app} is different from the exact angular spectrum C_ℓ^{ex} for the same initial spectrum. The errors caused by the approximation, or the relative differences between C_ℓ^{app} and C_ℓ^{ex} , are as large as about 30%. Thus, we should not use the observed power spectrum C_ℓ^{obs} directly in Eq. (10). Instead, we must find the C_ℓ^{app} that would be obtained for the actual $P(k)$. Of course, this is impossible in the rigorous sense, since it is the actual $P(k)$ that we are to reconstruct. It turns out to be possible, however, with accuracy high enough for our present purpose, because we find that the ratio,

$$b_\ell \equiv \frac{C_\ell^{\text{ex}}}{C_\ell^{\text{app}}}, \quad (13)$$

is almost independent of $P(k)$ (Matsumiya et al. 2003). Using this fact, we first calculate the ratio, $b_\ell^{(0)} = C_\ell^{\text{ex}(0)}/C_\ell^{\text{app}(0)}$, for a known fiducial initial spectrum $P^{(0)}(k)$ such as the scale-invariant one. Then, inserting $C_\ell^{\text{obs}}/b_\ell^{(0)}$, which is much closer to the actual C_ℓ^{app} , into the source term of Eq. (11), we may solve for $P(k)$ with good accuracy.

In practice, we cannot take the upper bound of the integration in the right-hand side of Eq. (11) to be infinite. The integrand in Eq. (11) is oscillating with its amplitude increasing with r . We therefore introduce a cutoff scale r_{cut} . However, this inevitably introduces a smoothing scale to our method. As the cutoff scale is made larger, the rapid oscillations of the integrand with increasing amplitude become numerically uncontrollable. On the other hand, if the cutoff scale is made smaller, the resolution in the k -space becomes worse as $\Delta k \simeq \pi/r_{\text{cut}}$. In the actual calculations, to maintain as good a numerical accuracy as possible and to obtain simultaneously as fine a resolution in k -space as possible, we convolve an exponentially decreasing function into the integration of the Fourier sine transform with the optimized cutoff scale of $r_{\text{cut}} \simeq 0.5d$, corresponding to $\theta \simeq 30^\circ$, or $\Delta \ell \sim 6$. Thus, the resolution of the Fourier sine transform is limited to $\Delta kd \simeq 6$. We could not adopt a finer resolution because of the numerical instability. Nevertheless, the resolution of our method is much finer than that of any other method. Note that there is an absolute theoretical limit $r_{\text{cut}} \lesssim 2d$, or $\Delta kd \gtrsim 1.5$, because of the finite size of the LSS sphere.

In this paper, we also account for the effect of observational errors on the reconstructed $P(k)$. First, for each ℓ we draw a random number from a Gaussian distribution whose mean value is equal to a central value of the observed C_ℓ and variance is given by the diagonal term of the covariance matrix, and then we reconstruct $P(k)$ from each simulated data set. In fact, each C_ℓ is weakly correlated with other multipoles and follows a χ^2 distribution. However, our procedure is valid because the correlation with other multipoles is weak enough and the χ^2 distribution is practically identical to the Gaussian distribution for sufficiently large ℓ where we analyze. We estimate the mean value and the variance of the reconstructed $P(k)$ at each k for 1000 realizations. We find that the intrinsic errors caused by our inversion method itself, whose magnitude is estimated by inverting C_ℓ spectra calculated from artificial $P(k)$ spectra without observational errors, are much smaller than the observational errors of WMAP, except around the singularities where the numerical errors are amplified.

To calculate C_ℓ^{ex} , we use a modified CMBFAST code with much finer resolutions than the original one in both k and ℓ . We limit C_ℓ in the range $20 \leq \ell \leq 700$ in order not to use data that have large observational errors due to the cosmic variance at small ℓ and the detector noise at large ℓ . We adopt the fiducial initial spectrum, $P^{(0)}(k)$, as the scale-invariant spectrum, and the fiducial cosmological parameter set as $h = 0.72$, $\Omega_b = 0.047$, $\Omega_\Lambda = 0.71$, $\Omega_m = 0.29$, and $\tau = 0.17$, which are the best-fit values to the WMAP data for the scale-invariant spectrum, $k^3 P(k) = A$. In this case, the positions of the singularities given by Eq. (12) are $kd \simeq 70, 430, 680, \dots$, where $d \simeq 1.34 \times 10^4 \text{Mpc}$. Because the reconstructed $P(k)$ around the singularities has large numerical errors that are amplified by the observational errors, we can obtain $P(k)$ with good accuracy in the limited range $120 \lesssim kd \lesssim 380$ or $9.0 \times 10^{-3} \text{Mpc}^{-1} \lesssim k \lesssim 2.8 \times 10^{-2} \text{Mpc}^{-1}$. Then, we vary some cosmological parameters to examine how the shape of the reconstructed $P(k)$ is affected. That is, we also calculate for some cases of $h = 0.65, 0.70, 0.75, 0.80$, $\Omega_b = 0.03, 0.04, 0.05, 0.06$, and $\Omega_\Lambda = 0.65, 0.70, 0.75, 0.80$, respectively. Note that since τ affects the shape of the power spectrum only on large scales, except for the normalization, we use a fixed value as $\tau = 0.17$.

3. Results and Discussion

3.1. Reconstruction from Original Data

We show $P(k)$ reconstructed from the WMAP data for the fiducial cosmological parameter set, namely, $h = 0.72$, $\Omega_b = 0.047$, $\Omega_\Lambda = 0.71$, $\Omega_m = 0.29$, and $\tau = 0.17$ in Fig. 1. We can see oscillations whose amplitude is about 20% – 30% of the mean value with frequency $(\Delta kd)^{-1} \simeq 1/15 - 1/10$. To check whether our method works correctly, we recalculate C_ℓ from the obtained $P(k)$ in the range $120 \lesssim kd \lesssim 380$, assuming scale-invariance outside of

this range, and compare it with the observational data of WMAP. As mentioned in Sec. 2, our method reconstructs $P(k)$ with a finite resolution, which is caused by the cutoff scale of the Fourier sine integral. In Fig. 2, we compare the cases of $r_{\text{cut}} \simeq 0.5d$ and $\simeq 0.3d$, which lead to $\Delta\ell \sim \Delta kd \simeq 6$ or $\Delta k \simeq 4.5 \times 10^{-4} \text{Mpc}^{-1}$, and $\Delta\ell \sim \Delta kd \simeq 10$ or $\Delta k \simeq 7.5 \times 10^{-4} \text{Mpc}^{-1}$, respectively. We find that the recalculated C_ℓ spectra agree with the binned WMAP data corresponding to the respective smoothing scales as shown in Fig. 3. These agreements are quite impressive. We also note that the characteristic frequency of oscillation changes accordingly as we vary the cutoff scale, so the observed oscillatory behavior with frequency $(\Delta kd)^{-1} \simeq 1/15 - 1/10$ in Fig. 1 does not necessarily have fundamental meaning. We confirm that the resolution becomes better as the cutoff scale is made larger, in agreement with the relation $\Delta k \simeq \pi/r_{\text{cut}}$. Of course, we adopt the former resolution, the finest possible scheme without numerical instability in subsequent sections.

3.2. Reconstruction from Binned Data

Figure 4 demonstrates the dependence of the reconstructed $P(k)$ on the bin size of the data. These $P(k)$ spectra are reconstructed from the binned WMAP data whose bin sizes are $\Delta\ell = 10, 20$, and 50 , by interpolating through the binned data points, respectively. This is to see both global and local features in $P(k)$. It is found that the oscillatory feature becomes more prominent as the bin size is made smaller, even if the spectrum globally looks scale-invariant. We emphasize that such nontrivial features cannot be quantified in $P(k)$ as long as conventional parameter-fitting methods are used.

3.3. Statistical Analysis

To examine whether the oscillatory features are real, we perform the following simulations and compare the results. First, we assume a scale-invariant $P(k)$ and calculate theoretical C_ℓ spectra for the fiducial cosmological parameter set. Then, we make artificial data of C_ℓ spectra with the same errors as those of the WMAP data by drawing random numbers. We use these artificial data to reconstruct $P(k)$, assuming that the cosmological parameters are known. The resultant $P(k)$ spectra for some different realizations are shown in Fig. 5. We can see that these reconstructed spectra also have oscillatory features whose amplitude and frequency are almost the same as the $P(k)$ from the WMAP data. This is caused purely by the scatter of the data. In other words, even if $P(k)$ is really scale-invariant, it is likely that the reconstructed $P(k)$ looks oscillatory because of the observational errors, and thus it is difficult to conclude whether or not there are some significant features in the

reconstructed $P(k)$ from the WMAP data. It is necessary to quantify their significance.

For this purpose, we define the deviation from the scale-invariance in $P(k)$ in the range between k_1 and k_2 as

$$D(k_1, k_2) \equiv \int_{k_1}^{k_2} dk [k^3 P(k) - A]^2, \quad (14)$$

and evaluate their statistical significance as follows. First, we calculate $D(k_1, k_2)$ for each reconstructed $P(k)$ from mock C_ℓ data for the scale-invariant $P(k)$ in the same simulation as mentioned above, with the fiducial cosmological parameters. Then, we estimate the probability that $D(k_1, k_2)$ for the simulation exceeds its observed value in the same range of k , by counting such events for 10,000 realizations. We show the results of this analysis in Table 1. It is found that only 1.41% of the simulations exceed the observed value in the range $100 \leq kd \leq 400$, and especially, only 0.39% in the range $175 \leq kd \leq 225$ and 0.59% in the range $325 \leq kd \leq 375$, from which we may conclude that there are some possible deviations around $kd \simeq 200$ and $\simeq 350$, as we can also see some prominent features in Fig. 1. This is consistent with Spergel et al. (2003), who show the contribution to χ^2 per multipole in C_ℓ after fitting the Λ CDM model with the power law $P(k)$ to the data.

3.4. Cosmological Parameters

As is seen in Fig. 1, the reconstructed $P(k)$ exhibits severe oscillations, reaching negative values locally around the singularity $kd \simeq 430$. One may wonder whether this is due to an inappropriate choice of the fiducial cosmological parameters, because if the different cosmological parameters from actual values are adopted in the inversion, the reconstructed $P(k)$ is distorted from the real one, especially around the singularities as shown by Matsumiya et al. (2003). We find, however, that 39.36% of the simulations based on the scale-invariant spectrum with the cosmological parameters fixed to the fiducial values result in larger values of $D(k_1, k_2)$ in the range $380 \leq kd \leq 430$. Hence, it is likely that the severe oscillations observed in Fig. 1 are not caused by an inappropriate choice of the cosmological parameters but are simply due to large observational errors. Still, it is important to see the dependence of the reconstructed $P(k)$ on the cosmological parameters, for the oscillatory features may change and we may be able to find a better choice of their values. In the ideal situations with sufficiently small observational errors, we may even constrain the cosmological parameters by requiring that the reconstructed $P(k)$ be positive definite.

Figure 6 depicts the dependence of the reconstructed $P(k)$ on the cosmological parameters. It is found that the oscillatory features remain, but the global amplitude and especially

the sharpness of the oscillations around the second singularity change. We also find some degree of degeneracy between h , Ω_b , and Ω_Λ . In Fig. 6, we can see that the increase in h has a similar effect as the decrease in Ω_b or Ω_Λ , that is, the amplitude of the oscillations increases similarly. This degeneracy, however, may be resolved if we could observe fine structures. For example, the reconstructed $P(k)$ is practically insensitive to h in the range $kd \lesssim 250$; hence, variation in h may be distinguished from that of Ω_b or Ω_Λ .

With the current magnitude of observational errors in C_ℓ , we encounter negative values of the reconstructed $P(k)$ for the scale-invariant spectrum. Hence, we need C_ℓ with smaller errors to apply this positivity criterion directly. In any case, we should examine $P(k)$ systematically for as many parameter sets as possible beyond those shown in Fig. 6, and we need a statistical method to quantify the positivity criterion in the presence of observational errors. This issue is currently under study.

At present, we can reconstruct $P(k)$ only in the range $100 \lesssim kd \lesssim 400$. If C_ℓ data improve at $\ell \gtrsim 700$, we will be able to obtain $P(k)$ up to the third singularity, $kd \simeq 680$. This additional information on $P(k)$ around the third singularity will be important for constraining the cosmological parameters, partly because of reduction in observational errors as discussed above and partly because the shape of $P(k)$ around the singularities is sensitive to the cosmological parameters, as mentioned in Sec. 3.3.

4. Conclusion

We have reconstructed the shape of the primordial spectrum, $P(k)$, from the WMAP angular power spectrum data, C_ℓ , by the inversion method proposed by Matsumiya et al. (2002, 2003), under the assumptions that the universe is spatially flat and the primordial fluctuations are purely adiabatic. First, we have set the cosmological parameters as $h = 0.72$, $\Omega_b = 0.047$, $\Omega_\Lambda = 0.71$, $\Omega_m = 0.29$, and $\tau = 0.17$. We have obtained an oscillatory $P(k)$. The amplitude of oscillations is about 20% – 30% of the mean value, and the frequency is about $(\Delta kd)^{-1} \simeq 1/15 - 1/10$, which reflects the resolution of our method. We have also confirmed that the reconstructed $P(k)$ has good accuracy in the range $120 \lesssim kd \lesssim 380$, or $9.0 \times 10^{-3} \text{Mpc}^{-1} \lesssim k \lesssim 2.8 \times 10^{-2} \text{Mpc}^{-1}$, with a resolution of $\Delta kd \simeq 5$, or $\Delta k \simeq 3.7 \times 10^{-4} \text{Mpc}^{-1}$. Thus, our inversion method can reconstruct $P(k)$ with a much finer resolution than other methods proposed so far, such as the binning, wavelet band powers, or direct wavelet expansion method (Wang et al. 1999a,b; Hannestad 2001, 2003; Wang and Mathews 2002; Bridle et al. 2003; Mukherjee and Wang 2003a,b,c).

To examine the statistical significance of possible nontrivial features in the reconstructed

spectrum, we have generated 10,000 sets of mock CMB data from the scale-invariant spectrum and reconstructed $P(k)$ from these artificial data. We have found that only 1.41% of them have the values of $D(k_1, k_2)$ larger than the observed value in the range $100 \leq kd \leq 400$, or $7.5 \times 10^{-3} \text{Mpc}^{-1} \lesssim k \lesssim 3.0 \times 10^{-2} \text{Mpc}^{-1}$, only 0.39% in the range $175 \leq kd \leq 225$, and 0.59% in the range $325 \leq kd \leq 375$. From these results we conclude that there are some possible deviations from scale-invariance around $kd \simeq 200$, or $k \simeq 1.5 \times 10^{-2} \text{Mpc}^{-1}$, and $kd \simeq 350$, or $k \simeq 2.6 \times 10^{-2} \text{Mpc}^{-1}$. On the other hand, we conclude that the severe oscillation of the reconstructed $P(k)$ around the singularity $kd \simeq 430$, which drives $P(k)$ to negative values in some regions, is due not to an inappropriate choice of the cosmological parameters but to the large observational errors. This is because we find a high probability around the singularity $kd \simeq 430$, or 39.36% in the range $380 \leq kd \leq 430$.

There are some issues that we plan to investigate in detail. First, it will be interesting to perform the reconstruction for a much wider range of the cosmological parameters and obtain systematic constraints on them, as mentioned in Sec. 3.4. Second, it may be necessary to apply the $D(k_1, k_2)$ test to other smooth forms of $P(k)$, for example, to those reconstructed from the binned data instead of the scale-invariant $P(k)$, as discussed in Sec. 3.2, for various values of the cosmological parameters. This is because the global shape of the reconstructed $P(k)$ changes depending on the cosmological parameters. Third, we should extend our formalism to include the CMB polarization so that it may be applied not only to the WMAP data but also to future CMB observations, such as Planck.² Inclusion of the CMB polarization will constrain $P(k)$ more severely, and if the B-mode polarization is detected, we can investigate the tensor mode of the primordial perturbations (Starobinsky 1979; Rubakov et al. 1982; Abbott and Wise 1984; Polnarev 1985; Crittenden et al. 1993a,b).

We would like to thank Eiichiro Komatsu for fruitful discussions. This work was supported in part by JSPS Grants-in-Aid for Scientific Research 12640269 (M.S.) and 13640285 (J.Y.) and by Monbu-Kagakusho Grant-in-Aid for Scientific Research (S) 14102004 (M.S.). N.K. is supported by Research Fellowships of JSPS for Young Scientists (04249).

REFERENCES

Abbott, L. F., and Wise, M. 1984, Nucl. Phys., B244, 541

²See <http://www.rssd.esa.int/index.php?project=PLANCK>

- Bennett, C. L., Banday, A. J., Gorski, K. M., Hinshaw, G., Jackson, P., Keegstra, P., Kogut, A., Smoot, G. F., Wilkinson, D. T., Wright, E. L. 1996, *ApJ*, 464, L1
- Bennett, C. L., Halpern, M., Hinshaw, G., Jarosik, N., Kogut, A., Limon, M., Meyer, S. S., Page, L., Spergel, D. N., Tucker, G. S., Wollack, E., Wright, E. L., Barnes, C., Greason, M. R., Hill, R. S., Komatsu, E., Nolte, M. R., Odegard, N., Peirs, H. V., Verde, L., Weiland J. L. 2003, *ApJS*, 148, 1
- Bi, X., Feng, B., and Zhang, X., hep-ph/0309195
- Bridle, S. L., Lewis, A. M., Weller, J., and Efstathiou, G. 2003, *Mon. Not. Roy. Astron. Soc.*, 342, L72
- Chung, D. J. H., Shiu, G., and Trodden, M. 2003, *Phys. Rev. D*, 68, 063501
- Cline, J. M., Crotty, P., and Lesgourgues, J. 2003, *JCAP*, 0309, 010
- Contaldi, C. R., Peloso, M., Kofman, L., and Linde, A. 2003, *JCAP*, 0307, 002
- Crittenden, R., Bond, J. R., Davis, R. L., Efstathiou, G., and Steinhardt, P. J. 1993a, *Phys. Rev. Lett.*, 71, 324
- Crittenden, R., Davis, R. L., and Steinhardt, P. J. 1993b, *ApJ*, 417, L13
- de Deo, S., Caldwell, R. R., and Steinhardt, P. J. 2003, *Phys. Rev. D*, 67, 103509
- de Oliveira-Costa, A., Tegmark, M., Zaldarriaga, M., and Hamilton, A., astro-ph/0307282
- Dvali, G., and Kachru, S., hep-ph/0310244
- Efstathiou, G. 2003a, *Mon. Not. Roy. Astron. Soc.*, 343, L95
- Efstathiou, G. 2003b, *Mon. Not. Roy. Astron. Soc.*, 346, L26
- Efstathiou, G. 2004, *Mon. Not. Roy. Astron. Soc.*, 348, 885
- Feng, B., Li, M., Zhang, R. J., and Zhang, X. 2003, *Phys. Rev. D*, 68, 103511
- Feng, B., and Zhang, X. 2003, *Phys. Lett.*, B570, 145
- Gaztañaga, E., Wagg, J., Multamäki, T., Montaña, A., and Hughes, D. H. 2003, *Mon. Not. Roy. Astron. Soc.*, 346, L47
- Hannestad, S. 2001, *Phys. Rev. D*, 63, 043009

- Hannestad, S., astro-ph/0311491
- Hu, W., and Sugiyama, N. 1995, ApJ, 444, 489
- Huang, Q. G., and Li, M. 2003, High Energy Phys., 06, 014
- Kawasaki, M., Yamaguchi, M., and Yokoyama, J. 2003, Phys. Rev. D, 68, 023508
- Kawasaki, M., and Takahashi, F. 2003, Phys. Lett., B570, 151
- Kodama, H., and Sasaki, M. 1984, Prog. Theor. Phys. Suppl., 78, 1
- Komatsu, E., Kogut, A., Nolta, M., Bennett, C. L., Halpern, M., Hinshaw, G., Jarosik, N., Limon, M., Meyer, S. S., Page, L., Spergel, D. N., Tucker, G. S., Verde, L., Wollack, E., Wright, E. L. 2003, ApJS, 148, 119
- Kyae, B., and Shafi, Q. 2003, JHEP, 0311, 036
- Matsumiya, M., Sasaki, M., and Yokoyama, J. 2002, Phys. Rev. D, 65, 083007
- Matsumiya, M., Sasaki, M., and Yokoyama, J. 2003, JCAP, 0302, 003
- Mukherjee, P., and Wang, Y. 2003a, ApJ, 593, 38
- Mukherjee, P., and Wang, Y. 2003b, ApJ, 598, 779
- Mukherjee, P., and Wang, Y. 2003c, ApJ, 599, 1
- Niarchou, A., Jaffe, A. H., and Pogosian, L. 2004, Phys. Rev. D, in press (astro-ph/0308461)
- Peiris, H. V., Komatsu, E., Verde, L., Spergel, D. N., Bennett, C. L., Halpern, M., Hinshaw, G., Jarosik, N., Kogut, A., Limon, M., Meyer, S., Page, L., Tucker, G. S., Wollack, E., Wright, E. L. 2003, ApJS, 148, 213
- Piao, Y., Feng, B., and Zhang, X., hep-th/0310206
- Polnarev, A. G. 1985, Sov. Astron., 29, 607
- Rubakov, V. A., Sazhin, M. V., and Veryaskin, A. V. 1982, Phys. Lett., B115, 189
- Shafieloo, A., and Souradeep, T., astro-ph/0312174
- Spergel, D. N., Verde, L., Peiris, H. V., Komatsu, E., Nolta, M. R., Bennett, C. L., Halpern, M., Hinshaw, G., Jarosik, N., Kogut, A., Limon, M., Meyer, S. S., Page, L., Tucker, G. S., Weiland, J. L., Wollack, E., Wright, E. L. 2003, ApJS, 148, 175

- Starobinsky, A. A. 1979, JETP Lett., 30, 682
- Tegmark, M., de Oliveira-Costa A., and Hamilton A. 2003, Phys. Rev. D, 68, 123523
- Tegmark, M., and Zaldarriaga, M. 2002, Phys. Rev. D, 66, 103508
- Uzan, J. P., Riazuelo, A., Lehoucq, R., and Weeks, J. 2004, Phys. Rev. D, 69, 043003
- Wang, Y., and Mathews, G. J. 2002, ApJ, 573, 1
- Wang, Y., Spergel, D. N., and Strauss, M. A. 1999a, in AIP Conf. Proc. 478, COSMO-98: Second International Workshop on Particle Physics and the Early Universe, ed. D. O. Caldwell (Woodbury: AIP), 164
- Wang, Y., Spergel, D. N., and Strauss, M. A. 1999b, ApJ, 510, 20
- Yamaguchi, M., and Yokoyama, J. 2003, Phys. Rev. D, 68, 123520
- Yokoyama, J. 1999, Phys. Rev. D, 59, 107303

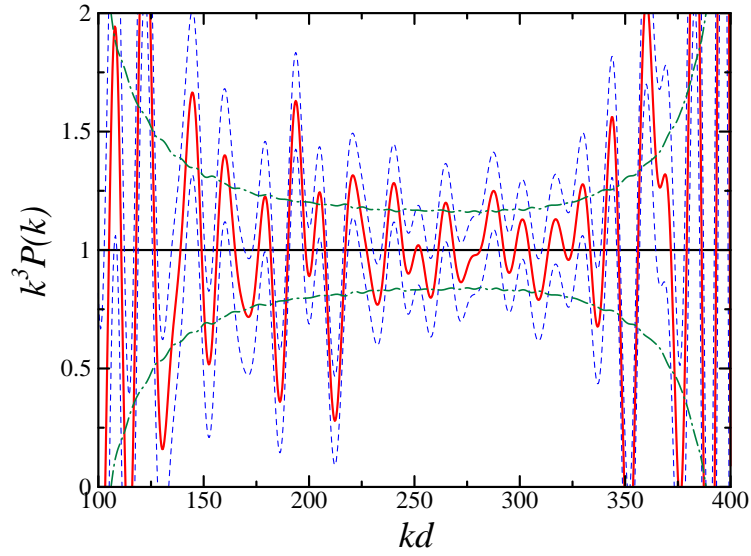


Fig. 1.— Primordial spectrum $P(k)$ reconstructed from the WMAP data for $h = 0.72$, $\Omega_b = 0.047$, $\Omega_\Lambda = 0.71$, $\Omega_m = 0.29$, and $\tau = 0.17$. The solid curve and the dashed curves represent the mean and the 1σ errors, respectively, of the reconstructed $P(k)$, while the dash-dotted curves represent the 1σ from the scale-invariance. The horizontal axis kd corresponds roughly to ℓ . The singularities lie at $kd \simeq 70$ and 430 . Some prominent features are seen around $kd \simeq 200$ and 350 .

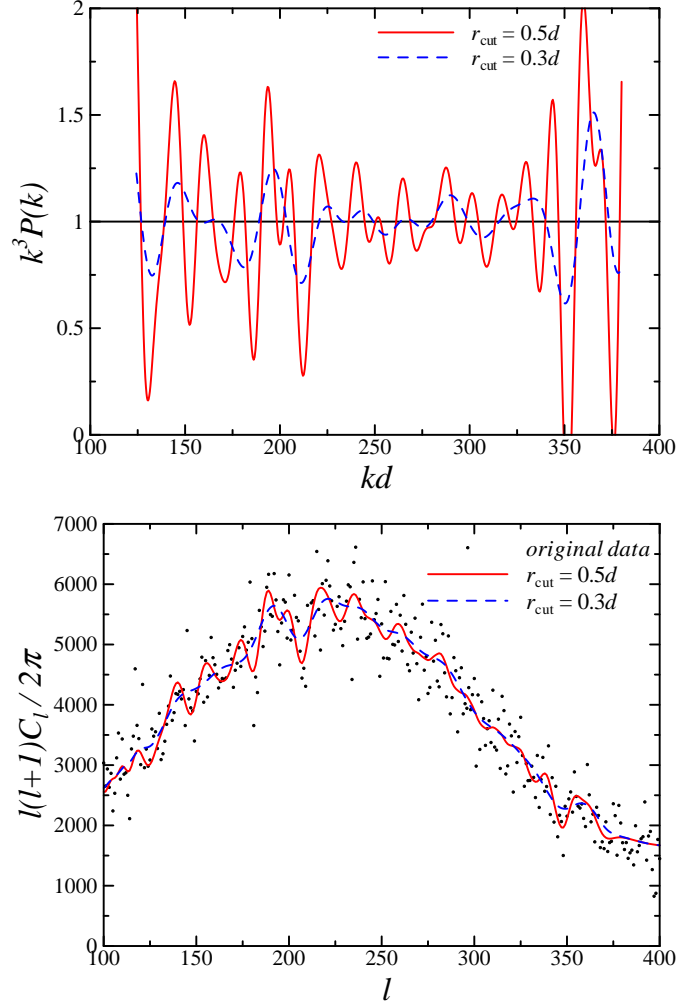


Fig. 2.— Dependence on the cutoff scale r_{cut} . *Top*: Reconstructed $P(k)$ spectra from the WMAP data for $r_{\text{cut}} \simeq 0.5d$ and $0.3d$. We see that the resolution becomes better as the cutoff scale is made larger. *Bottom*: Recovered C_ℓ spectra from the obtained $P(k)$ spectra.

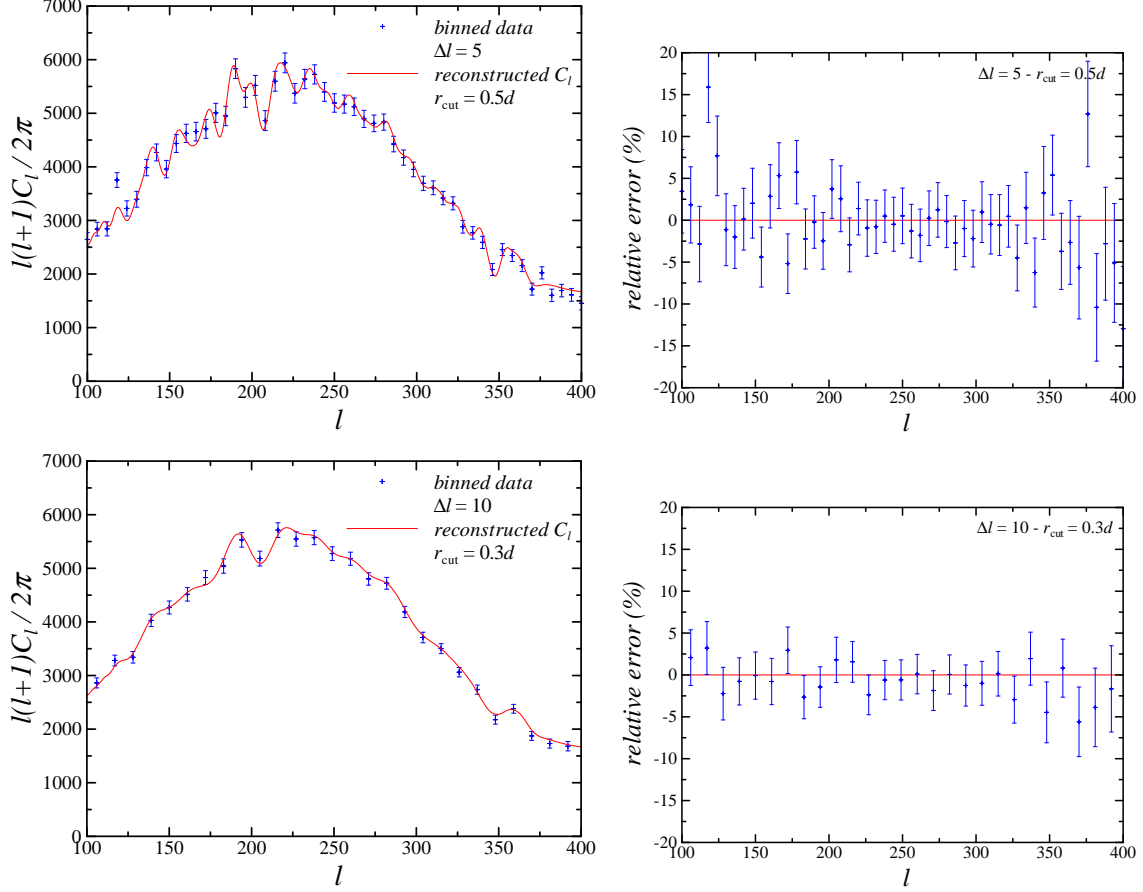


Fig. 3.— Accuracy check of our reconstruction method. We show the cases of $r_{\text{cut}} \simeq 0.5d$, which leads to $\Delta\ell \sim 6$ (top), and $r_{\text{cut}} \simeq 0.3d$, which leads to $\Delta\ell \sim 10$ (bottom), from the relation $\Delta\ell \sim \Delta kd \simeq \pi d/r_{\text{cut}}$. *Left:* Comparison of the binned WMAP data, C_ℓ^{bin} (plus signs with error bars), with the angular power spectrum, C_ℓ^{re} (solid curve), recovered from the reconstructed $P(k)$ shown in Fig. 2. *Right:* Relative errors, $(C_\ell^{\text{bin}} - C_\ell^{\text{re}})/C_\ell^{\text{re}}$. The relative errors are small for most of the bins except for those corresponding to the scales of the singularities.

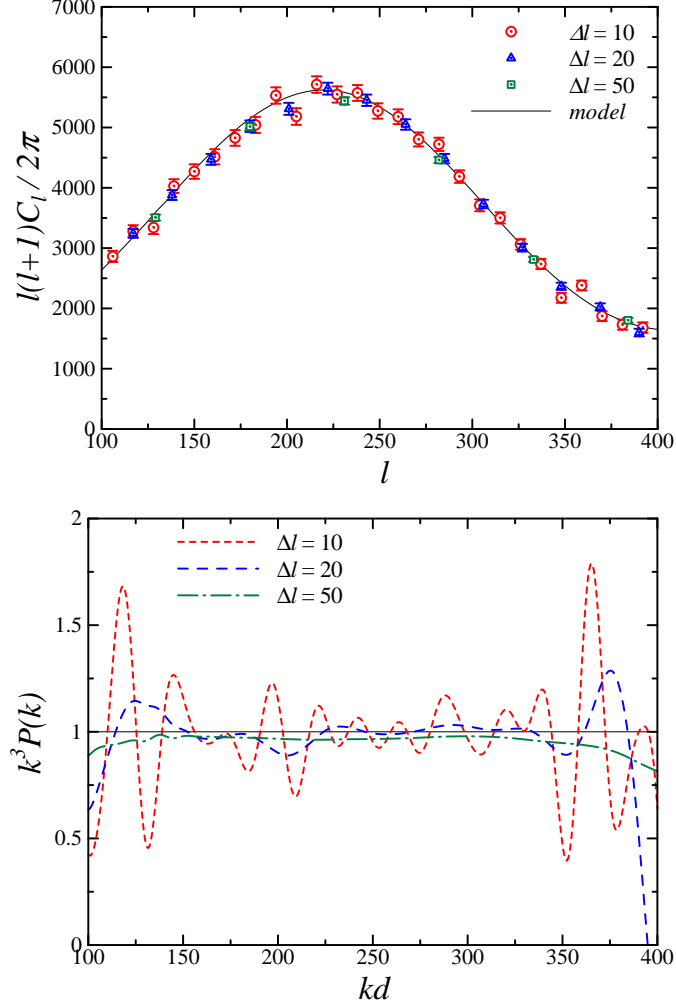


Fig. 4.— Reconstruction from the binned WMAP data. *Top*: Binned WMAP data whose bin sizes are $\Delta\ell = 10, 20$, and 50 ; the solid curve represents the fiducial model for the scale-invariant spectrum. *Bottom*: The $P(k)$ spectra reconstructed from the binned WMAP data. As the bin size is made smaller, we can see more oscillations.

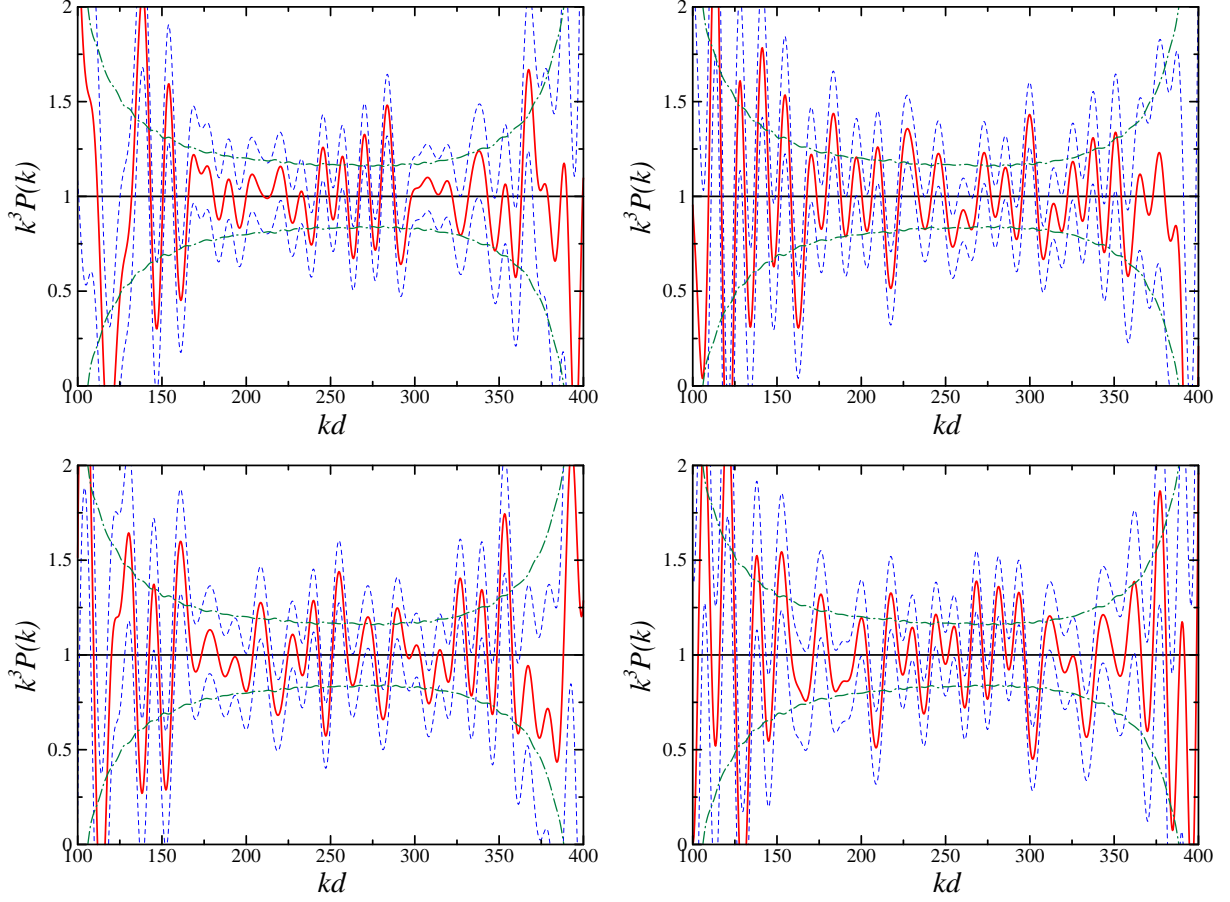


Fig. 5.— Primordial spectra $P(k)$ reconstructed from artificial CMB data for four different realizations. The original spectrum is taken to be scale invariant, and each realization is generated by drawing a random number to each C_ℓ with the same error as the WMAP data, assuming that the cosmological parameters are known. The same oscillatory features as shown in Fig. 1 are seen.

Table 1: Statistical Significance of the Deviations from the Scale Invariance

| range $[k_1d, k_2d]$ | [100,150] | [150,200] | [200,250] | [250,300] | [300,350] | [350,400] |
|----------------------|-----------|-----------|-----------|-----------|-----------|-----------|
| probability | 18.20% | 9.72% | 3.08% | 83.31% | 16.52% | 2.23% |

| range $[k_1d, k_2d]$ | [100,400] | [175,225] | [325,375] | [380,430] |
|----------------------|-----------|-----------|-----------|-----------|
| probability | 1.41% | 0.39% | 0.59% | 39.36% |

Note. — We show the probabilities that the deviation $D(k_1, k_2)$ for the simulation exceeds its observed value in various ranges $[k_1d, k_2d]$. The simulations are performed for the scale-invariant spectrum with the fiducial cosmological parameters, which are assumed to be known.

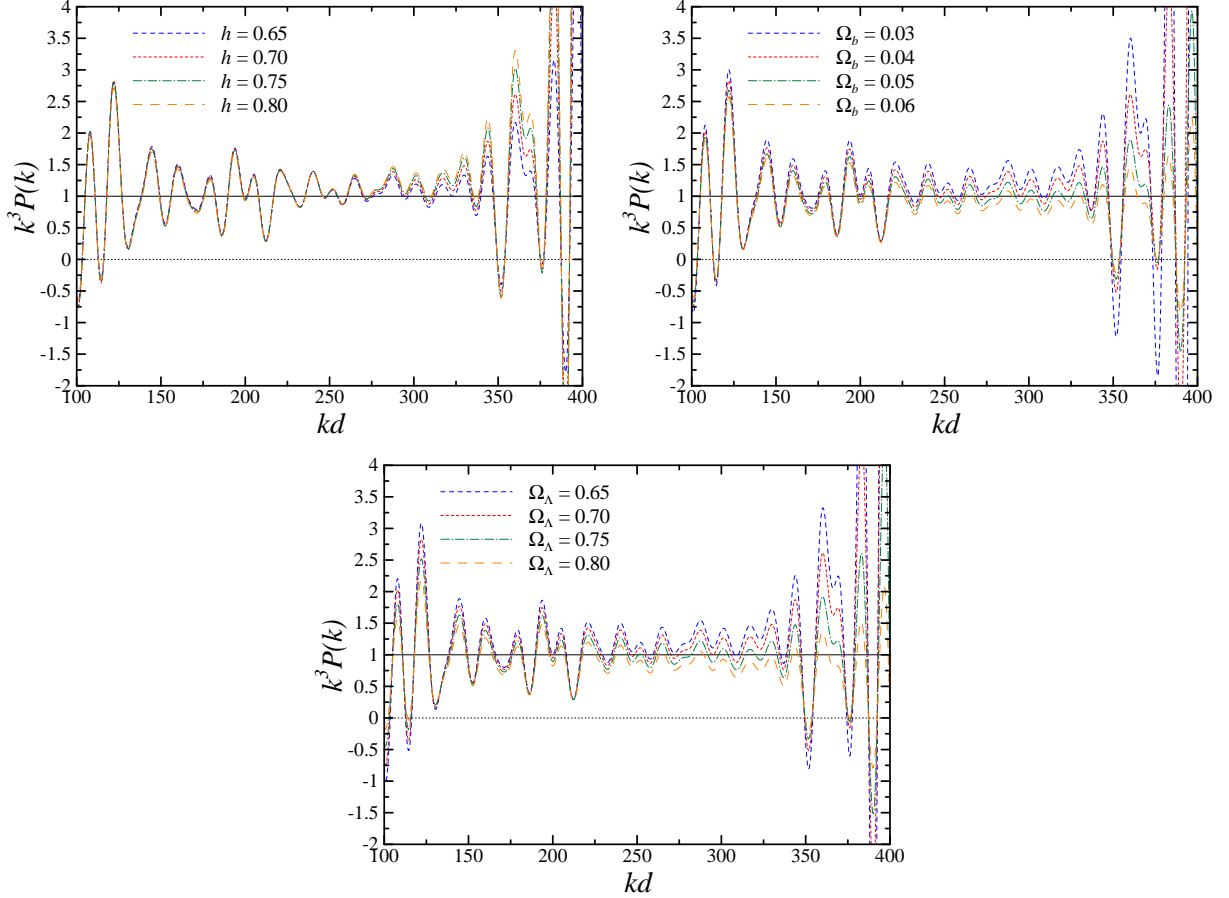


Fig. 6.— Some cases of different cosmological parameter sets. We show the reconstructed $P(k)$ from the WMAP data for $h = 0.65, 0.70, 0.75, 0.80$, $\Omega_b = 0.04$, $\Omega_\Lambda = 0.70$ (*top left panel*), $h = 0.70$, $\Omega_b = 0.03, 0.04, 0.05, 0.06$, $\Omega_\Lambda = 0.70$ (*top right panel*), and $h = 0.70$, $\Omega_b = 0.04$, $\Omega_\Lambda = 0.65, 0.70, 0.75, 0.80$ (*bottom panel*), respectively. The oscillatory features are roughly similar to each other throughout this range, but they are amplified around the second singularity in some cases.